Modeling of Hygrothermal Behavior of Two-Dimensional Concrete Structures

Dariusz J. Gawin, D.Sc. **Bernhard A. Schrefler, D.Sc.**

ABSTRACT

Coupled heat, air, and moisture transfer in concrete structures is of great practical importance in many fields of civil engineering. Modeling these phenomena, especially in fresh concrete structures or concrete elements exposed to fire, is a complex problem. Several nonlinear phenomena, such as heat and mass sources associated with hydration or dehydration processes, phase changes, hysteresis of sorption isotherms, material properties dependent on moisture content, and temperature and gas pressure, should be taken into account. A new two-dimensional finite element model of coupled heat, moisture, and air transfer in deforming porous building materials HMTRA is briefly presented. Different physical mechanisms governing the liquid and gas transport in the pores of partially saturated porous materials are clearly distinguished. Phase changes, hydration-dehydration processes, and related heat effects are taken into account as well. Temperature and moisture content dependent properties of the fluids and of the solid phase are considered. Also, the effect of material damaging on its intrinsic permeability is taken into account. This finite element model allows for the simulation of the evolution of temperature, gas pressure, moisture content, the global kinetics of the concrete maturing process, as well as stress and strain behavior. Some examples of computer simulations concerning hygrothermal behavior of two-dimensional concrete structures in various conditions are presented. Hygrothermal behavior of a matured concrete element, taking into account the hysteresis of sorption isotherms, is modeled. Temperature and moisture distribution in a fresh concrete structure and their influence on hydration process evolution are analyzed. Performance of a concrete element exposed to fire is simulated.

INTRODUCTION

Coupled heat, air, and moisture transfer in concrete structures is of great practical importance in many fields of civil engineering. Modeling these phenomena, especially in fresh concrete structures or concrete elements exposed to fire, is a complex problem. Several nonlinear phenomena (e.g., heat and mass sources associated with hydration or dehydration processes, phase changes, hysteresis of sorption isotherms, as well as permeability, porosity, and other material properties variable in time and dependent on temperature, gas pressure, and moisture content) should be taken into account in the simulation.

Mathematical models of these complex phenomena are obtained in two different ways, usually called phenomenological and mechanistic approach. Using the first one, heat and mass transport is described by means of a coupled, differential equation set of the diffusive type. Its coefficients are usually obtained by solving appropriate inverse problems that often result in a rather time-consuming experimental procedure. The model parameters are usually nonlinear functions of state variables because several complex physical phenomena are lumped together. Models of this type, widely used in practice, are aimed at predicting moisture content and temperature fields without entering in details of particular physical phenomena involved. Accuracy of the phenomenological models' predictions is good, as shown by many validation tests (Hens 1996). Examples of these types of models are the models by Bazant and Najjar (1972), TRATMO (Kohonen

Dariusz J. Gawin is an associate professor in the Department of Building Physics and Building Materials, Technical University of Lodz, Lodz, Poland. **Bernhard A. Schrefler** is a professor in the Department of Structures and Transportation Engineering, University of Padova, Padova, Italy.

1984), CHEAMOT (Gawin 1993), LATENITE (Karagiozis 1993), WUFI (Künzel 1994), and MOIST (Burch and Chi 1997). On the contrary, by using a mechanistic approach we model all main physical phenomena involved in hygrothermal behavior of materials; hence, equations of these models are usually much more complex. They are often obtained by use of the volume averaging theory (Whitaker 1977; Slattery 1981; Hassanizadeh and Gray 1979a, 1979b, 1980; Lewis and Schrefler 1998; Gawin 2000) or the theory of mixtures (de Boer et al. 1991). Parameters of these models have clear physical meaning and can be partly evaluated theoretically if the inner structure of the material is known (Auriault 1983; Auriault and Lewandowska 1997). In the last decade, the mechanistic approach was successfully applied for the analyses of many practical problems concerning coupled heat and moisture transfer in building materials (Häupl et al. 1997; Gawin et al. 1995, 2000), including such complex processes as hygrothermal behavior of concrete taking into account capillary hysteresis (Gawin et al. 2001a), performance of concrete structures during fire (Gawin et al. 1999, 2000), or maturing of concrete structures (Gawin 2000).

In this paper, some previous theoretical and numerical works of the authors are summarized, which together result in a new, more general mechanistic model of coupled heat and mass transfer in deforming porous building materials. Examples of application of this finite element model to simulations of hygrothermal behavior of concrete structures, including capillary hysteresis, material damaging at high temperature, and maturing of fresh concrete elements, are presented. In this paper hygrothermal performance of two-dimensional concrete structures is addressed and only some general indications concerning stress modeling are given. More information about the latter subject can be found in Lewis and Schrefler (1998) and Gawin et al. (1999, 2001b).

MATHEMATICAL MODEL

Wet concrete is modeled as a multiphase material, which is assumed to be in thermodynamic equilibrium state locally. The voids of the skeleton are filled partly with liquid water and partly with a gas phase.

The liquid phase consists of bound water, which is present in the whole range of moisture content, and capillary water, which appears when water content exceeds the upper limit of the hygroscopic region S_{ssp}. Moisture content is described here by the degree of saturation with water S_w related to the mass moisture content u_M ($kg_{water}/kg_{dry\_material}$) by the relation $S_w = (u_M \cdot \rho^s) / (n \cdot \rho^w)$, where n denotes porosity and ρ^w and ρ^s denote the densities of water and the solid skeleton, respectively. The gas phase is a mixture of dry air and water vapor (condensable constituent) and is assumed to be an ideal gas. The chosen primary variables of the model are gas pressure p^g, capillary pressure $p^c = p^g - p^w$ (p^w denotes water pressure), temperature T, displacement vector of the solid matrix $\mathbf{u}$, and degree of cement hydration Γ_{hydr} (when hydration or dehydration processes are analyzed). A physical explanation of our model, including the energy and mass transport mechanisms considered, can be found in Lewis and Schrefler (1998) and Gawin (2000).

The mathematical model consists of four balance equations. These equations were obtained in Lewis and Schrefler (1998) and Gawin (2000) by use of the volume averaging theory, also called hybrid mixture theory, developed by Hassanizadeh and Gray (1979a, 1979b, 1980). The mass balance of the dry air includes both diffusional and advectional (pressure forced) components of the mass fluxes,

$$-n\frac{\partial S_w}{\partial t} - \beta_s(1-n)S_g\frac{\partial T}{\partial t} + S_g div\,\boldsymbol{v}^s + \frac{S_g n}{\rho^a}\frac{\partial \rho^a}{\partial t} + \frac{1}{\rho^a} div\,\mathbf{J}_g^a + \frac{1}{\rho^a} div(nS_g\rho^a \boldsymbol{v}^{gs}) + \frac{(1-n)S_g}{\rho^s}\frac{\partial \rho^s}{\partial \Gamma_{hydr}}\frac{\partial \Gamma_{hydr}}{\partial t} = \frac{\dot{m}_{hydr}}{\rho^s}S_g, \tag{1}$$

and has been summed with the solid skeleton mass balance equation in order to eliminate the time derivative of porosity. Because of this, some terms related to thermal dilatation and mechanical deformation of the skeleton (the second and third terms on L.H.S.), as well as the mass source (sink) resulting from chemical reactions of the skeleton (hydration or dehydration), appear in Equation 1. The symbol t denotes time, $\dot{m}_{hydr}$ denotes mass source (sink) related to the hydration (dehydration) process, β_s is the cubic thermal expansion coefficient of the solid skeleton, $\mathbf{v}^{gs}$ denotes gas velocity relative to the solid skeleton, J_g^a denotes diffusional flux of the dry air, and the subscripts and superscripts s, w, a, v, and g are related to solid, liquid water, dry air, water vapor, and gas phase, respectively. According to the notation introduced by Hassanizadeh and Gray (1979a, 1979b, 1980), subscripts are used for physical quantities averaged in all phases of the medium, and superscripts for quantities averaged inside a single phase only.

The mass balances of liquid water and of vapor, summed together to eliminate the source term related to phase changes (evaporation-condensation or adsorption-desorption), form the mass balance equation of water species (Gawin 2000),

$$n(\rho^w - \rho^v)\frac{\partial S_w}{\partial t} - \beta_{swg}\frac{\partial T}{\partial t} + (\rho^v S_g + \rho^w S_w) div\,\boldsymbol{v}^s + S_g n\frac{\partial \rho^v}{\partial t} + div\,\mathbf{J}_g^v + div(nS_g\rho^v \boldsymbol{v}^{gs}) + div(nS_w\rho^w \boldsymbol{v}^{ws}) + \frac{(1-n)(S_g\rho^v + \rho^w S_w)}{\rho^s}\frac{\partial \rho^s}{\partial \Gamma_{hydr}}\frac{\partial \Gamma_{hydr}}{\partial t} = \frac{\rho^v S_g + \rho^w S_w - \rho^s}{\rho^s}\dot{m}_{hydr}, \tag{2}$$

$$\beta_{swg} = \beta_s(1-n)(S_g\rho^v + S_w\rho^w) + n\beta_w S_w\rho^w,$$

where $\mathbf{v}^{ws}$ denotes water velocity relative to the solid skeleton. As before, these balance equations are summed up with the solid phase mass conservation equation in order to eliminate the time derivative of porosity. As a result, several terms describing the skeleton deformations (hygrothermal and mechanical) and hydration (or dehydration) process appear in Equation 2.

The enthalpy conservation equation of the multiphase medium, obtained from the sum of the appropriate balance equations of the constituents, includes the heat effects due to phase changes and the hydration (dehydration) process, as well as the advectional and latent heat transfer,

$$\begin{aligned}(\rho C_p)_{ef}\frac{\partial T}{\partial t} + (\rho_w C_p^w \mathbf{v}^{ws} + \rho_g C_p^g \mathbf{v}^{gs}) \\ \cdot grad\ T - div(\lambda_{ef} grad\ T) \\ = -\dot{m}_{vap}\Delta H_{vap} + \dot{m}_{hydr}\Delta H_{hydr},\end{aligned} \tag{3}$$

where $(\rho C_p)_{ef}$ is effective thermal capacity, C_p is isobaric specific heat, λ_{ef} is effective thermal conductivity, ΔH_{vap} and ΔH_{hydr} are specific enthalpies of the phase change and the hydration (dehydration) process, and $\dot{m}_{vap}$ is the mass source or sink of vapor related to the evaporation (desorption) or condensation (adsorption) process.

In the hygroscopic moisture range, $S \leq S_{ssp}$, the terms in Equations 2 and 3, which describe the liquid phase, concern the bound water and, thus, ΔH_{vap} should be substituted by ΔH_{ads} (i.e., enthalpy of adsorption). In Equation 3, the phase change term has been substituted using the liquid water mass balance equation.

Introducing Bishop's stress tensor σ'', also called effective stress tensor (Lewis and Schrefler 1998), responsible for all the deformations of a concrete, the linear momentum conservation equation of the whole medium is given by (Gawin 2000),

$$\begin{aligned}div[\sigma'' - \mathbf{I}(p^g - p_{atm} - S_w p^c)] \\ + [(1-n)\rho^s + nS_w\rho^w + nS_g\rho^g]\ \mathbf{g} = 0,\end{aligned} \tag{4}$$

where p_{atm} is atmospheric pressure, $\mathbf{I}$ is the unit, second order tensor, and $\mathbf{g}$ is the acceleration of gravity.

The evolution equation for the degree of cement hydration appearing in Equation 2 has the form,

$$\Gamma_{hydr} = \Gamma_{hydr}(t_{eq}), \tag{5}$$

where the equivalent period of hydration, t_{eq}, is given by (Bazant 1988):

$$t_{eq}(t) = \int_o^t \beta_T(\tau)\beta_\varphi(\tau)d\tau, \tag{6}$$

with

$$\beta_T(\tau) = \exp\left[\frac{U_{hydr}}{R}\left(\frac{1}{T_o} - \frac{1}{T(\tau)}\right)\right], \tag{7a}$$

$$\beta_\varphi(\tau) = \{1 + \alpha^4[1 + \varphi(\tau)]^4\}^{-1}. \tag{7b}$$

U_{hydr} denotes activation energy of hydration, R is the universal gas constant (U_{hydr}/R = 2700 K), T_o is the reference temperature, and $\alpha \cong 5$ (Bazant 1988).

When the dehydration process at high temperature is analyzed, because of its irreversible nature, one can assume that (Gawin et al. 1999)

$$\Gamma_{hydr} = \Gamma_{hydr}(T_{max}), \tag{8}$$

where $T_{\max}(t)$ is the highest temperature reached by the concrete till time instant t.

The governing Equations 1 through 8 are completed by an appropriate set of constitutive and state equations, as well as some thermodynamic relationships.

The constitutive relationship for the solid skeleton in the following form,

$$d\sigma'' = \mathbf{C}_T(d\varepsilon - d\varepsilon_T - d\varepsilon_0), \tag{9}$$

is assumed together with the definition of the strain matrix $\mathbf{B}$ relating strain tensor ε and displacement vector $\mathbf{u}$,

$$\varepsilon = \mathbf{B}\ u, \tag{10}$$

where $\boldsymbol{C}_T$ is the tangent matrix, $d\varepsilon_T = \mathbf{I}\ \beta_s/3\ dT$ is the strain caused by thermo-elastic expansion, and $d\varepsilon_0$ represents the autogeneous strain increment and the irreversible part of the thermal strain. We would like to underline that Equations 4 and 10 also take into account effect of the hygral state changes (described by capillary pressure p^c and degree of saturation S_w) on deformations and stresses of the material.

Fresh concrete is modeled as a viscoelastic material using the solidification theory by Bazant and Prasannan (1989a, b). In this theory, concrete maturing is attributed to a growth of the volume fraction of load-bearing hydrated cement, which itself is considered as a non-aging viscoelastic material.

During analysis of concrete behavior at high temperature, the material damage caused by the development of cracks is considered following the theory of scalar isotropic damage by Mazars and Pijaudier-Cabot (1989). This theory defines a modified effective stress $\tilde{\sigma}$ and takes into account the damage D ($0 \leq D \leq 1$) as a parameter measuring the reduction of resistant area due to the crack beginning and spreading,

$$\tilde{\sigma} = \sigma''\frac{A}{\tilde{A}} = \frac{\sigma''}{1-D} \tag{11}$$

where damage depends on the value of equivalent strain reached by the medium, considering its irreversible character (Mazars and Pijaudier-Cabot 1989). A is the resistant area of the uncracked material, whereas $\tilde{A}$ is the resistant area of the damaged material. The applied damage theory was obtained by use of a phenomenological approach. It is slightly inconsistent with the rest of our mechanistic model, but we have found this theory very suitable for numerical analyzing of the damage response of concrete.

As a constitutive equation for the capillary water, Darcy's law is applied,

$$\boldsymbol{v}_{ws} = \frac{k^{rw}\mathbf{k}}{\mu^{w}}[grad\ p^{c} - grad\ p^{g} + \rho^{w}\mathbf{g}], \tag{12}$$

and similarly for the gas phase, i.e.,

$$\boldsymbol{v}_{gs} = -\frac{k^{rg}\mathbf{k}}{\mu^{g}}[grad\ p^{g} - \rho^{g}\mathbf{g}], \tag{13}$$

where $\mathbf{k}$ is the intrinsic permeability tensor, and k^{rg} and k^{rw} are values of relative permeability of the gaseous and liquid phases, while μ^{g} and μ^{w} are their dynamic viscosities.

For the physically adsorbed water flow, the following constitutive law is applied,

$$\mathbf{v}_{ws} = -\mathbf{D}_{b}\ grad\ S_{w}, \tag{14}$$

where $\mathbf{D}_b$ is the bound water diffusion tensor and $S_w(p^c)$ is the degree of saturation with bound water, which is assumed to be constant in the capillary moisture range.

For the description of the diffusion process in the binary gas mixture of dry air and water vapor, Fick's law is applied,

$$\mathbf{J}_{g}^{v} = -\rho^{g}\frac{M_{a}M_{w}}{M_{g}^{2}}\mathbf{D}_{g}^{v}\ grad\left(\frac{p^{v}}{p^{g}}\right) = -\mathbf{J}_{g}^{a}, \tag{15}$$

where M_a, M_w, and M_g are molar masses of dry air, water vapor, and the gas phase, and D_g^v is the effective diffusivity tensor of vapor in the air.

The equation of state of perfect gases and Dalton's law are assumed for dry air, water vapor, and their mixture (moist air):

$$\begin{aligned} p^{a} &= \rho^{a}TR/M_{a}, \qquad & p^{g} &= p^{a} + p^{v}, \\ p^{v} &= \rho^{v}TR/M_{w}, \qquad & \rho^{g} &= \rho^{a} + \rho^{v}, \end{aligned} \tag{16}$$

where

$$M_{g} = \left(\frac{\rho^{v}}{\rho^{g}}\frac{1}{M_{w}} + \frac{\rho^{a}}{\rho^{g}}\frac{1}{M_{a}}\right)^{-1}. \tag{17}$$

Due to the curvature of the meniscus separating the liquid water from the gas phase inside the pores of the concrete, which is considered as a capillary porous body, the equilibrium water vapor pressure p^v differs from the saturation pressure p^{vs} and may be obtained from the Kelvin equation,

$$p^{v} = p^{vs}(T) \cdot \exp\left(-\frac{p^{c}M_{w}}{\rho^{w}RT}\right), \tag{18}$$

where the water vapor saturation pressure p^{vs}, depending only upon temperature T, may be calculated from the Clausius-Clapeyron equation or from empirical correlations (e.g., the formula of Hyland and Wexler [ASHRAE 1997]). Equation 18 is valid both for the capillary and adsorbed water (Lewis and Schrefler 1998). In the latter case, the capillary pressure p^c should be understood as a thermodynamic potential, referring to the bound water and cannot be identified to the pressure.

For model closure, it is further necessary to define the initial and boundary conditions. The initial conditions specify the full fields of gas pressure, capillary pressure, temperature, and displacements in the whole analyzed domain Ω and its boundary Γ ($\Gamma = \Gamma_{\pi} \cup \Gamma_{\pi}^{q}$, π=g, c, t, u):

$$p^{g} = p_{o}^{g}, \quad p^{c} = p_{o}^{c}, \quad T = T_{o}, \quad \mathbf{u} = \mathbf{u}_{o}, \quad \text{for } t = 0. \tag{19}$$

The boundary conditions can be of Dirichlet's type on Γ_g:

$$\begin{aligned} p^{g}(t) &= \hat{p}^{g}(t) \text{ on } \Gamma_{g}, \\ p^{c}(t) &= \hat{p}^{c}(t) \text{ on } \Gamma_{c}, \\ T(t) &= \hat{T}(t) \text{ on } \Gamma_{t}, \\ \hat{\boldsymbol{u}}(t) &= \hat{\boldsymbol{u}}(t) \text{ on } \Gamma_{u}, \end{aligned} \tag{20}$$

or of Neumann's (Equations 21a and 21d) and Robin's (Equations 21b,c) type on Γ_{π}^{q}:

$$\left[\rho^{a}\frac{\mathbf{k}k^{rg}}{\mu^{g}}(-grad\ p^{g} + \rho^{g}\mathbf{g}) + \rho^{g}\frac{M_{a}M_{w}}{M_{g}^{2}}\mathbf{D}_{g}^{v}\ grad\left(\frac{p^{v}}{p^{g}}\right)\right] \cdot \mathbf{n} = q^{a}, \text{ on } \Gamma_{g}^{q}, \tag{21a}$$

$$\left[\rho^{w}\frac{\mathbf{k}k^{rw}}{\mu^{w}}(-grad\ p^{g} + grad p^{c} + \rho^{w}\mathbf{g}) + \rho^{v}\frac{\mathbf{k}k^{rg}}{\mu^{g}}(-grad\ p^{g} + \rho^{g}\mathbf{g}) - \rho^{g}\frac{M_{a}M_{w}}{M_{g}^{2}}\mathbf{D}_{g}^{v}grad\left(\frac{p^{v}}{p^{g}}\right)\right] \cdot \mathbf{n} = q^{w} + q^{w} + \beta_{c}(\rho^{v} - \rho_{\infty}^{v}), \qquad \text{on } \Gamma_{c}^{q}, \tag{21b}$$

$$\left(\rho^{w}\frac{\mathbf{k}k^{rw}}{\mu^{w}}(-grad\ p^{g} + grad\ p^{c} + \rho^{w}\mathbf{g})\Delta H_{vap} - \lambda_{ef}\ grad\ T\right) \cdot \mathbf{n} = q^{T} + \alpha_{c}(T - T_{\infty}) + e\sigma_{o}(T^{4} - T_{\infty}^{4}), \qquad \text{on } \Gamma_{t}^{q}, \tag{21c}$$

$$\boldsymbol{\sigma} \cdot \boldsymbol{n} = \bar{\boldsymbol{t}}, \qquad \text{on } \Gamma_{u}^{q} \tag{21d}$$

where $\mathbf{n}$ is the unit normal vector, pointing toward the surrounding gas; q^a, q^v, q^w, and q^T are, respectively, the imposed fluxes of dry air, vapor, liquid water, and the imposed heat flux; $\bar{t}$ is the imposed traction; ρ_{∞}^{v} and T_{∞} are the mass concentration of water vapor and the temperature in the far field of undisturbed gas phase; e is emissivity of the interface; σ_o is the Stefan-Boltzmann constant, and α_c and β_c are convective heat and mass transfer coefficients.

The mathematical model (Equations 1 through 21) contains several material parameters, which should be determined experimentally. However, indispensable experimental effort in this case is smaller in comparison to similar phenomenological models because effect of moisture content (saturation degree) and/or temperature and/or gas pressure on most of the transport properties can be predicted theoretically (Lewis and Schrefler 1998; Gawin et al. 1999; Gawin 2000). Despite

this, experimental verification of the mechanistic models is necessary. Some data concerning the verification of our model can be found in Gawin (2000) and Gawin et al. (2001c).

NUMERICAL SOLUTION

Discretization in space of the governing equations is carried out by means of the finite element method (e.g., Zienkiewicz and Taylor 1989, 1991). The unknown variables are expressed in terms of their nodal values as

$$\begin{aligned} p^g(t) &= \mathbf{N}_p \bar{\mathbf{p}}^g(t), \qquad & p^c(t) &= \mathbf{N}_p \bar{\mathbf{p}}^c(t), \\ T(t) &= \mathbf{N}_t \bar{\mathbf{T}}(t), \qquad & \boldsymbol{u}(t) &= \mathbf{N}_u \bar{\mathbf{u}}(t). \end{aligned} \tag{22}$$

The variational (weak) form of the heat and mass transfer equations, applying also the other ones required to complete the model, was obtained by means of Galerkin's method (weighted residuals) and can be expressed in matrix form as

$$\begin{bmatrix} \mathbf{K}_{gg} & \mathbf{K}_{gc} & \mathbf{K}_{gt} & 0 \\ \mathbf{K}_{cg} & \mathbf{K}_{cc} & \mathbf{K}_{ct} & 0 \\ \mathbf{K}_{tg} & \mathbf{K}_{tc} & \mathbf{K}_{tt} & 0 \\ \mathbf{K}_{ug} & \mathbf{K}_{uc} & \mathbf{K}_{ut} & \mathbf{K}_{uu} \end{bmatrix} \begin{Bmatrix} \bar{\mathbf{p}}^g \\ \bar{\mathbf{p}}^c \\ \bar{\mathbf{T}} \\ \bar{\mathbf{u}} \end{Bmatrix} + \begin{bmatrix} \mathbf{C}_{gg} & \mathbf{C}_{gc} & \mathbf{C}_{gt} & \mathbf{C}_{gu} \\ \mathbf{0} & \mathbf{C}_{cc} & \mathbf{C}_{ct} & \mathbf{C}_{cu} \\ \mathbf{0} & \mathbf{C}_{tc} & \mathbf{C}_{tt} & \mathbf{C}_{tu} \\ \mathbf{0} & \mathbf{0} & \mathbf{0} & \mathbf{0} \end{bmatrix} \frac{\partial}{\partial t} \begin{Bmatrix} \bar{\mathbf{p}}^g \\ \bar{\mathbf{p}}^c \\ \bar{\mathbf{T}} \\ \bar{\mathbf{u}} \end{Bmatrix} = \begin{Bmatrix} \mathbf{f}_g \\ \mathbf{f}_c \\ \mathbf{f}_t \\ \mathbf{f}_u \end{Bmatrix}. \tag{23}$$

The matrices occurring in Equation 23 are listed in Gawin (2000). The above nonsymmetric, nonlinear, and coupled system of partial differential equations may be rewritten in compact form as

$$\mathbf{K}(\mathbf{x})\mathbf{x} + \mathbf{C}(\mathbf{x})\frac{\partial \mathbf{x}}{\partial t} = \mathbf{f}(\mathbf{x}) \tag{24}$$

where $\mathbf{x}^{\mathbf{T}} = \left\{ \bar{\mathbf{p}}^{\mathbf{g}}, \bar{\mathbf{p}}^{\mathbf{c}}, \bar{\mathbf{T}}, \bar{\mathbf{u}} \right\}$ and the nonlinear (matrix) coefficients $\mathbf{C}(\mathbf{x})$, $\mathbf{K}(\mathbf{x})$, and $\mathbf{f}(\mathbf{x})$, obtained by assembling the submatrices indicated in Equation 23, are given in Gawin (2000).

The time discretization is accomplished through a fully implicit finite difference scheme (backward difference),

$$\mathbf{C}_{n+1}\frac{\mathbf{x}_{n+1} - \mathbf{x}_n}{\Delta t} + \mathbf{K}_{n+1}\mathbf{x}_{n+1} - \mathbf{f}_{n+1} = \mathbf{0} \tag{25}$$

where $\mathbf{C}_{n+1} = \mathbf{C}(\mathbf{x}_{n+1})$, $\mathbf{K}_{n+1} = \mathbf{K}(\mathbf{x}_{n+1})$, $\mathbf{f}_{n+1} = \mathbf{f}(\mathbf{x}_{n+1})$, n is the time step number, and Δt is the time step length.

Because of the nonlinearity of Equation 25, the solution is obtained with a Newton-Raphson type procedure,

$$\left[\left(\frac{\partial \mathbf{C}}{\partial \mathbf{x}} \right)_{n+1}^{k} \frac{\mathbf{x}_{n+1}^{k} - \mathbf{x}_n}{\Delta t} + \frac{\mathbf{C}_{n+1}^{k}}{\Delta t} + \left(\frac{\partial \mathbf{K}}{\partial \mathbf{x}} \right)_{n+1}^{k} \mathbf{x}_{n+1}^{k} + \mathbf{K}_{n+1}^{k} - \left(\frac{\partial \mathbf{f}}{\partial \mathbf{x}} \right)_{n+1}^{k} \right] \Delta \mathbf{x}_{n+1}^{k+1} = - \left[\mathbf{C}_{n+1}^{k} \frac{\mathbf{x}_{n+1}^{k} - \mathbf{x}_n}{\Delta t} + \mathbf{K}_{n+1}^{k} \mathbf{x}_{n+1}^{k} - \mathbf{f}_{n+1}^{k} \right] \tag{26}$$

where k is the iteration index and, at the end of each iteration, the primary variables are updated as follows:

$$\mathbf{x}_{n+1}^{k+1} = \mathbf{x}_{n+1}^{k} + \Delta \mathbf{x}_{n+1}^{k+1} \tag{27}$$

A special "switching" procedure (Gawin and Schrefler 1996), allowing one to deal with fully and partially saturated media present at the same time in the different parts of the domain, is applied. Based on the discretization presented, the HMTRA research computer code has been developed for the solution of the nonlinear and nonsymmetrical system of equations governing heat and mass transfer in deformable concrete at high temperature.

SIMULATION OF HYGROTHERMAL BEHAVIOR OF CONCRETE STRUCTURES IN VARIOUS CONDITIONS

The finite element model HMTRA, based on the theory presented in the previous section, was successfully applied for analysis of several problems concerning hygrothermal behavior and deformations of soils (Gawin and Schrefler 1996; Lewis and Schrefler 1998), building materials (Gawin et al. 1996, 2000; Gawin 2000), concrete elements taking into account capillary hysteresis (Gawin 2000; Gawin et al. 2001a), fresh concrete components (Gawin 2000), and concrete structures at high temperatures (Gawin et al. 1998, 1999). Following are some examples showing the application of the code for simulations of two-dimensional concrete components in the latter three mentioned situations, which are rather difficult from the theoretical and numerical point of view.

In all the examples presented in this section, isotropic properties of concrete are assumed (i.e., tensors $\mathbf{k}$, $\mathbf{D}_b$, $\mathbf{D}_g^v$, λ_{ef} are substituted by the appropriate coefficients multiplied by the unit tensor of the second order).

Simulation of Capillary Hysteresis in Concrete

The hygrothermal behavior of a concrete cylinder with diameter of 16 cm and height of 30 cm is simulated by use of the HMTRA-ANN code, which uses an artificial neural network (ANN) for description of sorption isotherms with capillary hysteresis (Gawin et al. 2001a). The experimental sorption data, concerning primary adsorption and desorption curves for normal concrete with water–cement ratio w/c = 0.7 (Hedenblad 1996), have been applied for training of the ANN using the back propagation algorithm. Generally speaking, at the moment there is a lack of experimental data on inner adsorption and desorption curves of building materials. Here,

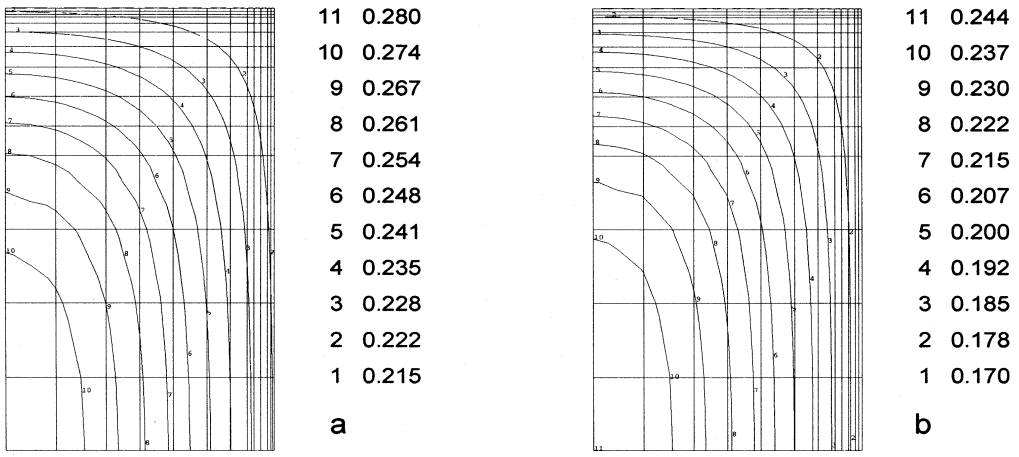

Figure 1 *The resulting distributions of water saturation at time instant t = 168 hours for the analyzed cases: a) with hysteresis and b) without hysteresis.*

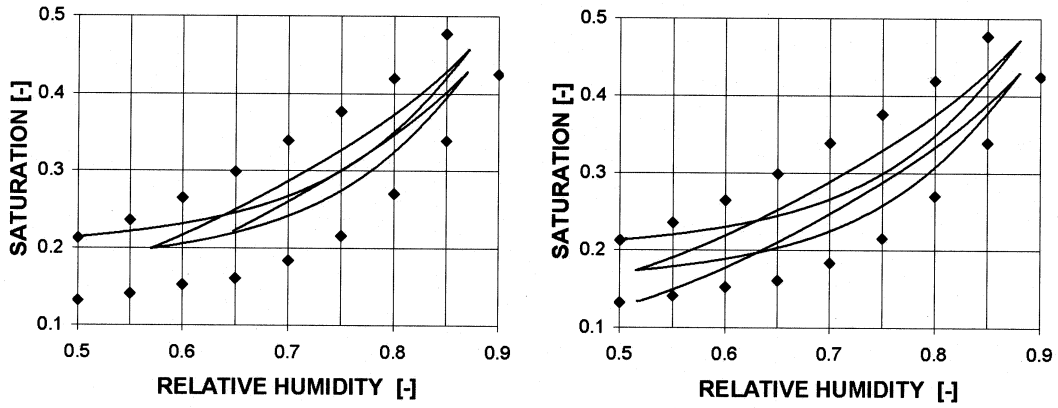

Figure 2 *The resulting relative humidity-water saturation changes for the analyzed case with hysteresis: a) in the corner and b) in the center of the concrete cylinder.*

these inner curves have been created in an artificial way. More information about their modeling can be found in Gawin et al. (2001a) and physical phenomena related to sorption and hysteresis are described in Gregg and Sing (1982).

The following material data are used in computations: ρ_o = 2330 kg/m^3, n = 0.1, λ_{ef} = 1.67 W/(m·K), C_{ap} = 940 J/(kg·K), $k = 10^{-19}$ m^2, and $\beta_s = 0.9 \cdot 10^{-6}$ 1/K. Young's modulus E = 14 GPa, Poisson's ratio ν = 0.25, and Biot's constant α = 0.5 are assumed.

Initially, the element has temperature T_0 = 278.15 K and relative humidity φ_0 = 50% RH. The external surfaces of the cylinder are exposed to convective boundary conditions for heat and moisture exchange. Temperature and relative humidity of the surrounding air change harmonically with the period T = 168 hours (one week), temperature between T_{min} = 278.15 K and T_{max} = 298.15 K, and relative humidity between φ_{min} = 50% RH and φ_{max} = 90% RH. The corresponding convective heat and mass transfer coefficients are β_c=0.02 m/s and α_c=23 W/(m^{2}K). The gas pressure of the air is assumed to be constant, p^g = 101325 Pa. For all surfaces, except those exposed to convective heat and moisture exchange, all the normal fluxes and normal displacements are set to zero. The total simulation time comprised two full wetting-drying cycles.

One-quarter of the cylinder has been spatially discretized by use of 168 8-node serendipity elements (12 along the radius and 14 along the height, i.e., 557 nodes). During computations, various time steps (from 1 second up to 100 seconds) according to the stage of the process evolution are applied. The problem is solved for isotherms with and without hysteresis (for the main desorption curve). The resulting distributions of water saturation at time instant t = 168 hours for the two cases are presented in Figure 1. In Figure 2, the hysteresis loops for the first case (for the points in the corner and in the center of the cylinder), obtained using the saturation and relative humidity results for the same time instants, are shown. Additionally, the experimental data of the primary adsorption and

desorption curves (diamond points) are shown in the figure. The time evolutions of temperature and relative humidity in the center of the cylinder are compared in Figure 3. A small effect of the hysteresis on the temperature solution is obtained. This is caused by a relatively weak dependence of the thermal conductivity upon the concrete moisture content. Hence, some differences in the material moisture content (saturation degree) had a very small influence on the temperature solution.

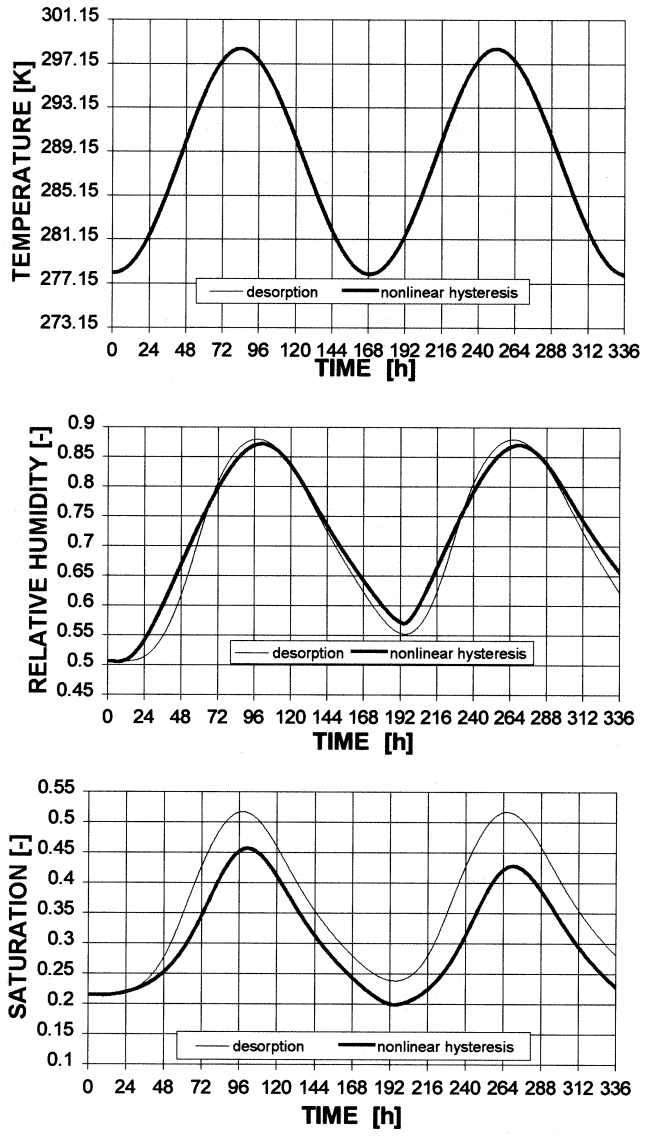

Figure 3 *The resulting temperature, relative humidity, and water saturation evolutions in the center of the concrete cylinder for the case with capillary hysteresis.*

Simulation of a UHPC Concrete Nuclear Waste Container at High Temperature

Hygrothermal behavior and material damage of a cylindrical UHPC concrete nuclear waste container (diameter of 100 cm, height of 150 cm, wall thickness of 12 cm) during fire is solved. The analyzed UHPC has the following material parameters: ρ_o = 2470 kg/m^3, λ_{ef} = 2.32 W/(m·K), n = 0.044, $k_o = 10^{-20}$ m^2, f_c = 200 MPa, E = 55.2 GPa, and ν = 0.18.

Considering the shape of the sample, one-half of the container is discretized by 268 axisymmetric eight-node elements (10 × 14 for the bottom and 8 × 16 for the wall). Initially, the specimen is at capillary pressure p^c = 92.67 MPa and at temperature T = 293.15 K. The external temperature increases according to the standard ISO fire conditions, while the partial vapor pressure of the external air has constant value p^v = 1000 Pa. The problem is solved for an unsealed heated surface, assuming the radiative boundary conditions for heat exchange with $e\sigma_o = 5.1\ 10^{-8}$ W/(m^2·K^4) and convection for mass exchange with β_c = 0.019 m/s. For the inner, unheated surfaces of the container, the convective boundary conditions for heat and mass exchange with α_c = 18 W/(m^2·K) and β_c = 0.019 m/s are assumed. The greatest changes are observed in the corner of the container where the gas pressure and temperature reach the highest values; hence, only results for this zone are presented in Figures 4 through 7.

Figures 4a and 4b show the distributions of temperature at time stations 4 minutes and 8 minutes (i.e., the final time of simulation). A front of the increasing temperature and decreasing saturation with liquid water, moving from the heated surface toward the internal surface, can be observed in Figures 5 a and 5b. The vapor pressure distributions at the same time stations are shown in Figures 6a and 6b. The maximum vapor pressure is observed very close to the external corner, reaching at the end a very high value of p^v = 14.4 MPa. At the same time, this zone damage parameter reaches a value greater than 0.95 (Figure 7), which indicates a high probability of spalling phenomenon occurrence.

Simulation of Maturing Process of a Concrete Column

Hygrothermal behavior of a concrete column (60 cm × 40 cm) during the first 30 days of its maturing in ambient air of different relative humidities is simulated by use of the HMTRA-HC code (Gawin 2000). The heat and mass sources related to the concrete maturing process are expressed as a function of the hydration degree $\Gamma_{hydr}(t_{eq})$. Effect of the temperature and relative humidity on the time evolution of the cement hydration (Equations 5 through 7) is taken into account using experimental data for the cement type IV given in Neville (1995).

The following material data are used in computations: ρ_o = 1900 kg/m^3, n = 0.1, λ_{ef} = 1.67 W/(m·K), C_{ap} = 940 J/(kg·K), $k = 10^{-18}$ m^2, $\beta_s = 0.9 \cdot 10^{-6}$ 1/K, E = 55

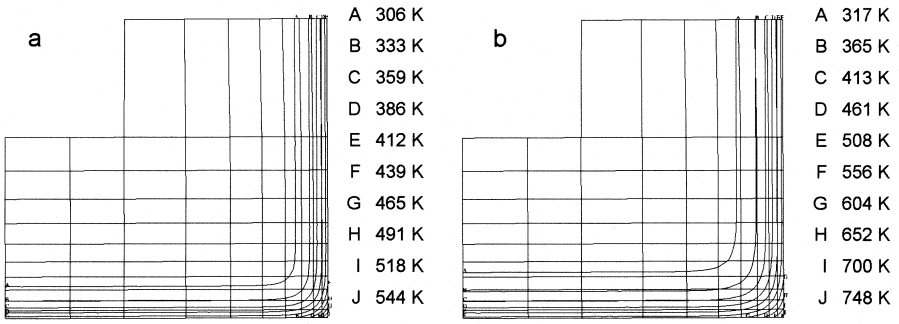

Figure 4 *Resulting temperature distribution in the heated UHPC concrete nuclear waste container at different time instants: a) t = 4 min, b) t = 8 min.*

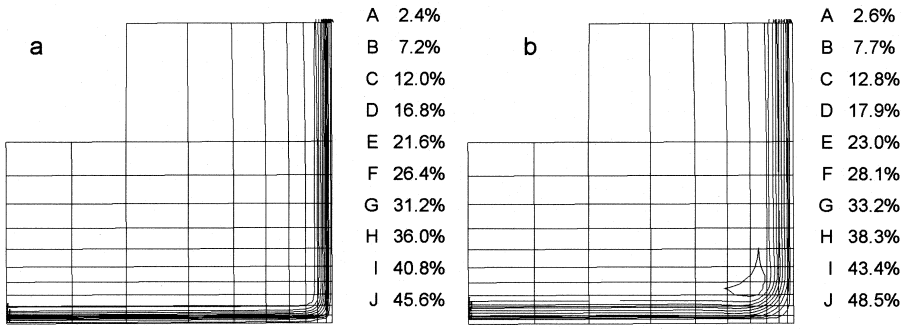

Figure 5 *Resulting saturation distribution in the heated UHPC concrete nuclear waste container at different time instants: a) t = 4 min, b) t = 8 min.*

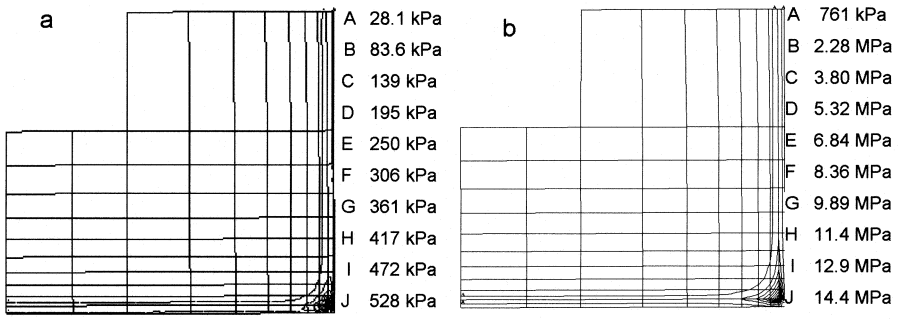

Figure 6 *Resulting vapor pressure distribution in heated UHPC concrete nuclear waste container at different time stations: a) t = 4 minutes, b) t = 8 minutes.*

GPa, and ν = 0.25. Initially, the column has a temperature T_0 =293.15 K and relative humidity φ_0=99.9%. It is assumed that the hydration process started 2.5 hours before; hence, the element already has a certain shape rigidity. The external surfaces of the column are exposed to convective boundary conditions for heat and moisture exchange. The temperature and relative humidity of the surrounding air are constant: T_∞ = 293.15 K and φ = 95% or 55%. The convective heat and mass transfer coefficients are assumed as β_c = 0.033 m/s and α_c = 8.3 W/(m^{2}K). For all surfaces, except those exposed to convective heat and moisture exchange, the normal displacements and normal fluxes are set to zero.

Because of the symmetry, only one-quarter of the column has been spatially discretized by use of 130 eight-node serendipity elements (13 × 10, i.e., 437 nodes). During computations, various time steps (from 10 seconds up to 900 seconds) are used according to the stage of the process evolution. The resulting distributions of the temperature at time instant t = 24 hours and total displacements (negative values correspond to the element shrinkage) at t = 720 hours for the two analyzed cases of relative humidity are presented in Figures 8 and 9. In Figure 10, the time evolutions of the temperature, relative humidity, and hydration degree in the center and the corner of the cylinder are compared for the two cases. They show a considerable effect of the ambient relative humidity upon the kinetics of hydration process and hygrothermal state of the maturing concrete, especially during first hours of the process. Self-desiccation and self-heating phenomena, characteristics of fresh concrete, are clearly visible, influencing significantly the deformations of the column. For the analyzed column, the hydration degree and the relative humidity for both analyzed cases have almost the same value inside the element and close to its surfaces.

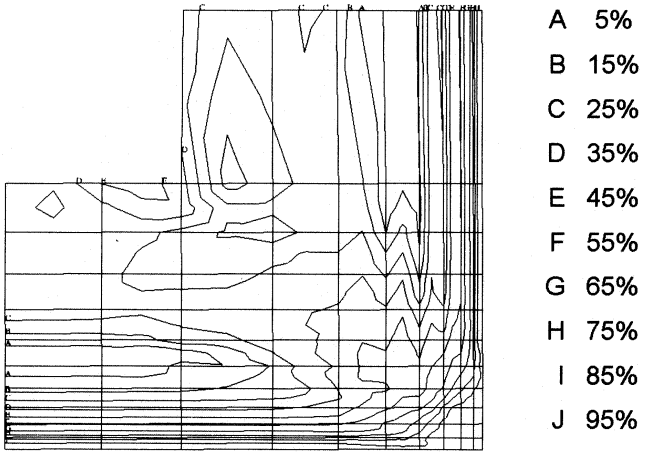

Figure 7 *Resulting damage distribution in heated UHPC concrete nuclear waste container at time station t = 8 minutes.*

CONCLUSIONS

HMTRA, the finite element model of coupled heat, moisture, and air transfer in porous building materials has been presented. It takes into account all important mass and energy transport mechanisms, phase changes, capillary hysteresis, and material deformations. It allows for analysis of hygrothermal behavior of two-dimensional (also axisymmetric) concrete structures in various situations, including concrete maturing and performance at high temperature, as well as evaluation of material stresses, deformations, or damage (crack development). Three examples of application of the

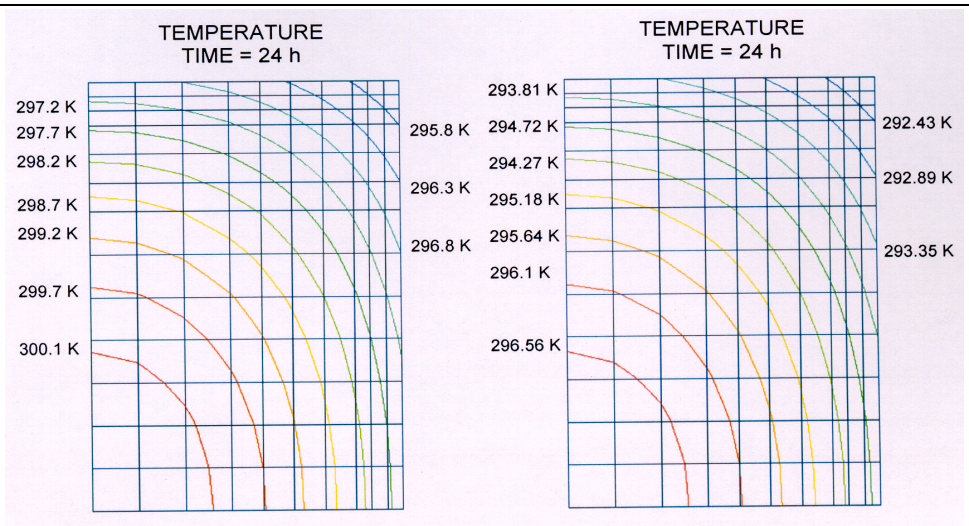

Figure 8 *The distributions of temperature in concrete column maturing in ambient air having a) 95% RH, b) 55% RH, at time instant t = 24 hours.*

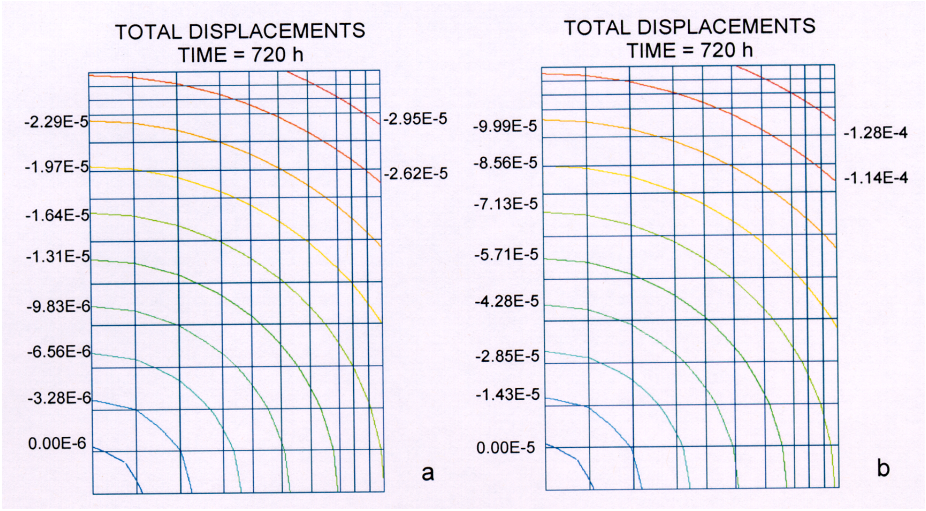

Figure 9 *The distributions of total displacements in concrete column maturing in ambient air having a) 95% RH, b) 55% RH, at time instant t = 24 hours.*

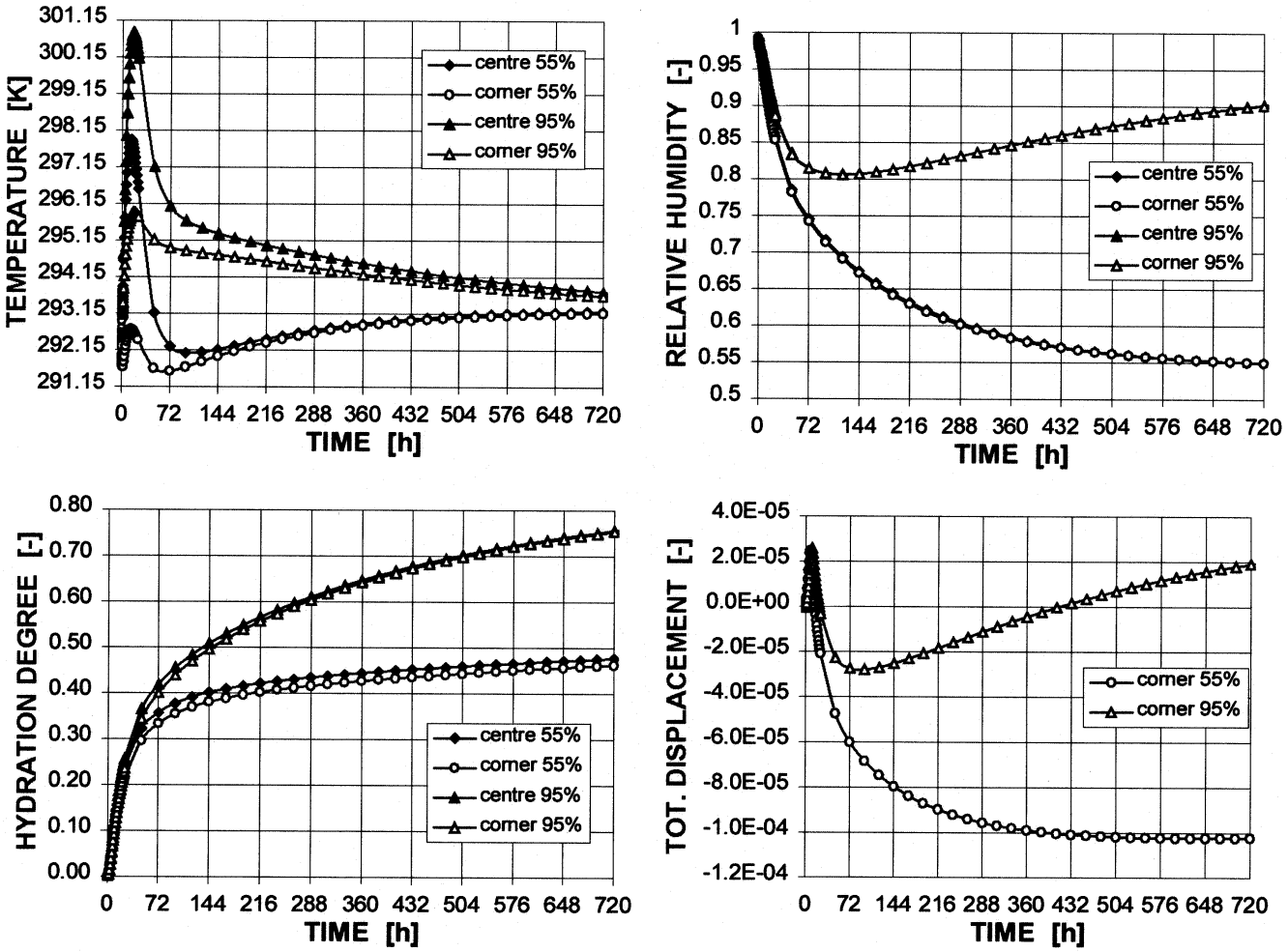

Figure 10 *Comparison of the time evolutions of the temperature, relative humidity, hydration degree, and total displacements in the center and in the corner of the concrete cylinder maturing in ambient with the two different values of the relative humidity.*

model for analysis of the performance of concrete structures, including their hygrothermal state, deformations, and damage, show the versatility of the model.

ACKNOWLEDGMENTS

The first author's research was partly supported by the Polish State Committee for Scientific Research (K.B.N.) grant No. 7 T07E 018 19.

REFERENCES

Auriault, J.-L. 1983. Effective macroscopic description for heat conduction in periodic composites. *J. Heat Mass Transfer* 25: 861-869.

Auriault, J.-L., and J. Lewandowska. 1997. Effective diffusion coefficient: from homogenisation to experiment. *Transport in Porous Media* 27: 205-223.

ASHRAE. 1997. *1997 ASHRAE Handbook—Fundamentals*. Atlanta: American Society of Heating, Refrigerating and Air-Conditioning Engineers, Inc.

Bazant, Z.P. (ed.). 1988. *Mathematical modeling of creep and shrinkage of concrete*. Chichester: Wiley.

Bazant, Z.P., and L.J. Najjar. 1972. Nonlinear water diffusion in nonsaturated concrete. *Matériaux et Constructions* (Paris), Vol. 5: 3-20.

Bazant, Z.P., and S. Prasannan. 1989a. Solidification theory for concrete creep. I: Formulation. *J. Eng. Mech.* 115 (8): 1691-1703.

Bazant, Z.P., and S. Prasannan. 1989b. Solidification theory for concrete creep. II: Verification and Application. *J. Eng. Mech.* 115 (8): 1704-1725.

de Boer, R., W. Ehlers, S. Kowalski, and J. Plischka. 1991. *Porous media, a survey of different approaches*. *Forschungsbericht aus dem Fachbereich Bauwesen*, Vol. 54. Essen: Universität-Gesamthochschule Essen.

Burch, D.M., and J. Chi. 1997. *A PC program for predicting heat and moisture transfer in building envelopes, release 3.0*. NIST Special Publication 917. Gaithersburg, Md. National Institute of Standards and Technology.

Gawin, D. 1993. A numerical solution of coupled heat and moisture transfer problems with phase changes in porous building materials. *Archives of Civil Engng*. 39 (4): 393-412.

Gawin, D. 2000. *Modelling of coupled hygro-thermal phenomena in building materials and building components, Scientific Bulletin of Lódz Technical University, Dissertations Series No.279* (in Polish). Editions of Lódz Technical University, Lódz.

Gawin, D., P. Baggio, and B.A. Schrefler. 1995. Coupled heat, water and gas flow in deformable porous media. *Int. J. Num. Meth. in Fluids* 20: 969-987.

Gawin, D., P. Baggio, and B.A. Schrefler. 1996. Modelling heat and moisture transfer in deformable porous building materials. *Arch. of Civil Engineering* 42: 325-349.

Gawin, D., J. Kosny, and A. Desjarlais. 2000. The effect of moisture content on accuracy of the steady state thermal conductivity tests for light- weight concretes. *Proceedings of ACEEE Summer Study on Energy Efficient Economy, Monterey, Calif*. (CD ROM).

Gawin, D., M. Lefik, and B.A. Schrefler. 2001a. ANN approach to sorption hysteresis within a coupled hygro-thermo-mechanical FE analysis. *Int. J. Num. Meth. Engng*. 50: 299-323.

Gawin, D., F. Pesavento, and B.A. Schrefler. 2001b. Simulation of damage—Permeability coupling in hygro-thermo-mechanical analysis of concrete at high temperature. *Comm. Num. Meth. Engng*. (in print).

Gawin, D., F. Pesavento, and B.A. Schrefler. 2001c. *Modelling of hygro-thermal behaviour and damage of concrete at temperature above critical point of water* (submitted for publication).

Gawin, D., C.E. Majorana, and B.A. Schrefler. 1999. Numerical analysis of hygro-thermic behaviour and damage of concrete at high temperature. *Mech. Cohes.-Frict. Mat.* 4: 37-74.

Gawin, D., C.E. Majorana, F. Pesavento, and B.A. Schrefler. 1998. A fully coupled multi-phase FE model of hygro-thermo-mechanical behaviour of concrete at high temperature. In Onate and Idelsohn (eds.), *Computational mechanics. New trends and applications*. *Proceedings IV World Congress on Computational Mechanics in Buenos Aires*. Barcelona: CIMNE (CD).

Gawin, D., and B.A. Schrefler. 1996. Thermo-hydro-mechanical analysis of partially saturated porous materials. *Engineering Computations* 13 (7): 113-143.

Gregg, S.J., and K.S.W. Sing. 1982. *Adsorption, surface area and porosity*, 2d ed. London: Academic Press.

Häupl, P., J. Grunewald, H. Fechner, and H. Stopp. 1997. Coupled heat, air and moisture transfer in building structures. *Int. J. Heat Mass Transfer* 40 (7): 1633-1642.

Hassanizadeh, S.M., and W.G. Gray. 1979a. General conservation equations for multi-phase systems: 1. Averaging procedure. *Adv. Water Resources* 2:131-144.

Hassanizadeh, S.M., and W.G. Gray. 1979b. General conservation equations for multi-phase systems: 2. Mass, momenta, energy and entropy equations. *Adv. Water Resources* 2:191-203.

Hassanizadeh, S.M., and W.G. Gray. 1980. General conservation equations for multi-phase systems: 3. Constitutive theory for porous media flow. *Adv. Water Resources* 3:25-40.

Hedenblad, G. 1996. *Materialdata för Fukttransportberäkningar* (in Swedish). Stockholm: Byggfor-skningsradet.

Hens, H. 1996 *Heat, air and moisture transfer in insulated envelope parts. Final Report, Vol.1, Task1: Modelling. Common exercises*. Energy Conservation in Buildings and Community Systems Programme, International Energy Agency.

Karagiozis, A.N. 1993. *Overview of the 2-D hygro-thermal heat moisture transport model LATENITE*. Internal IRC/BPL Report.

Kohonen, R. 1984. A method to analyze the transient hygrothermal behaviour of building materials and components. Ph. D. dissertation, VTT, Publications 21, Espoo, Finland.

Künzel, H.M. 1994. *Verfahren zur ein- and zweidimensionalen Berechnung des gekoppelten Wärme- and Feuchtetransports in Bauteilen mit einfachen Kennwerten*. Dissertation, Universität Stuttgart, Stuttgart.

Lewis, R.W., and B.A. Schrefler. 1998. *The finite element method in the static and dynamic deformation and consolidation of porous media*, 2d ed. Chichester: Wiley.

Mazars, J., and J. Pijaudier-Cabot. 1989. Continuum damage theory—Application to concrete. *J. of Eng. Mechanics*, ASCE 115 (2): 345-365.

Neville, A.M. 1995. *Properties of concrete, Fourth and final ed.* Harlow: Longman House.

Slattery, J.C. 1981. *Momentum, energy and mass transfer in continua*. R.E. Krieger, Florida.

Whitaker, S. 1977. Simultaneous heat, mass and momentum transfer in porous media: A theory of drying. *Advances in Heat Transfer* 13:119-203.

Zienkiewicz, O.C., and R.L. Taylor. 1989. *The finite element method*, Vol. 1, 4th ed. London: Mc Graw Hill.

Zienkiewicz, O.C., and R.L. Taylor. 1991. *The finite element method*, Vol. 2, 4th ed. London: Mc Graw Hill.